Molecular Cell, Vol. 5, 411–421, March, 2000, Copyright ©2000 by Cell Press

The RFX-Type Transcription Factor DAF-19 Regulates Sensory Neuron Cilium Formation in *C. elegans*

Peter Swoboda,* Haskell T. Adler, and James H. Thomas
Department of Genetics
University of Washington
Seattle, Washington 98195

Summary

Many types of sensory neurons contain modified cilia where sensory signal transduction occurs. We report that the *C. elegans* gene *daf-19* encodes an RFX-type transcription factor that is expressed specifically in all ciliated sensory neurons. Loss of *daf-19* function causes the absence of cilia, resulting in severe sensory defects. Several genes that function in all ciliated sensory neurons have an RFX target site in their promoters and require *daf-19* function. Several other genes that function in subsets of ciliated sensory neurons do not have an RFX target site and are not *daf-19* dependent. These results suggest that expression of the shared components of sensory cilia is activated by *daf-19*, whereas cell-type-specific expression occurs independently of *daf-19*.

Introduction

Polarized cells such as epithelial cells and neurons create functional compartments by localizing proteins to specialized regions in the cell. Proteins such as channels and receptors are placed and maintained in these distinct compartments, and this spatial arrangement is crucial for cell function. Ciliated sensory endings are one such functional compartment. Motile cilia line various epithelia, such as those in the respiratory tract and oviduct, where they sweep fluids or small particles along the surface. In contrast, sensory cilia are typically nonmotile. Instead, they provide a compartment for the localization and exposure of signal transduction proteins to incoming sensory signals.

Specialized vertebrate sensory cilia include those in the outer segments of the rod and cone photoreceptor cells in the eye, the kinocilia associated with the stereocilia of the hair cells in the ear, and the olfactory cilia of the sensory neurons in the nose. In the nematode *C. elegans*, 60 of the 302 neurons of the hermaphrodite are ciliated sensory neurons (Ward et al., 1975; Ware et al., 1975; Perkins et al., 1986; White et al., 1986; Hall and Russell, 1991). Apart from these, there are no other ciliated cells in *C. elegans*. The 60 ciliated neurons comprise 24 distinct neuron classes with many structurally distinct types of sensory cilia. They function in the reception of chemo- and mechanosensory stimuli. The importance of cilia for sensory transduction is evidenced in *C. elegans* by the fact that mutants with structurally abnormal cilia are defective in chemosensation and in some forms of mechanosensation (Perkins et al., 1986; Kaplan and Horvitz, 1993; Bargmann and Mori, 1997; Driscoll and Kaplan, 1997).

The architecture of cilia and of their close structural relatives, flagella, has been well documented (Perkins et al., 1986; Johnson, 1995; Stephens, 1995). The core of cilia and flagella consists of a microtubular axoneme enclosed by a membrane. A number of their protein components have been found using biochemical and genetic approaches (Dutcher, 1995; Stephens, 1995). However, relatively little is known about the mechanisms by which cilia and flagella are generated and shaped, and how their structural components are assembled.

RFX-type transcription factors are found widely in eukaryotic organisms. Five RFX family members each have been identified from mice and humans (RFX1–RFX5) (Emery et al., 1996a), and one member each from *S. pombe* (sak1) (Wu and McLeod, 1995) and *S. cerevisiae* (Crt1) (Huang et al., 1998). RFX-type transcription factors are defined by a characteristic DNA binding domain (DBD) which is distinct from any other described DBD (Reith et al., 1990; Reith et al., 1994; Emery et al., 1996b). Some members of the RFX family also have a dimerization domain (DIM) that is specific for RFX-type transcription factors (Emery et al., 1996a). Specific roles of RFX-type transcription factors have been described only for RFX5 in humans and for Crt1 in *S. cerevisiae*. They act as transcriptional activators or repressors by binding to specific sequences (X boxes; RFX = *r*egulatory *f*actor binding to the *X* box) in promoters of target genes. Human RFX5 is the DNA- binding subunit of a nuclear complex that is essential for the transcription of MHC class II genes in the immune response (Mach et al., 1996). In *S. cerevisiae*, Crt1 acts as a repressor in the DNA damage and replication checkpoint pathways. In response to DNA damage or replication block, binding of Crt1 to X box sequences is abolished, resulting in transcriptional derepression of its target genes (Huang et al., 1998).

We report the isolation and characterization of *daf-19*, the sole *C. elegans* member of the RFX family. We show that *daf-19* is expressed in ciliated sensory neurons during the time period when cilia are generated. Loss of *daf-19* function results in the absence of sensory cilia. We found putative target sites (X boxes) for DAF-19 in promoters of several genes required for normal sensory cilium formation. We demonstrate in vivo that the expression of this group of genes is regulated by *daf-19* in an X box–dependent manner. We propose that during ciliated sensory neuron differentiation *daf-19* initiates the cascade of events that generates ciliated endings.

Results

Phenotypic Characterization of *daf-19* Mutants

daf-19 mutations were identified in screens for constitutive dauer larva formation (Daf-c phenotype) (Malone and Thomas, 1994; D. Riddle, personal communication;

*To whom correspondence should be addressed (e-mail: peter@genetics.washington.edu).

Table 1. Percent Dauer Formation of *daf-19* Mutant Animals[a]

Genotype	15°C	20°C	25°C
Wild type	0 (many)	0 (many)	0 (many)
daf-19 (m86)	67 (340)	85 (216)	98 (310)
daf-19 (sa190)	76 (184)	91 (213)	94 (235)
daf-19 (sa232)	70 (335)	69 (245)	94 (242)

[a] The number of animals counted is given in parentheses.

Experimental Procedures). The dauer larva is an arrested alternative larval stage capable of enduring harsh environmental conditions. When conditions improve, the dauer larva recovers and resumes normal development to reproductive adulthood. Entry into and exit from the dauer stage depend on amphid sensory neurons (Bargmann and Mori, 1997; Riddle and Albert, 1997). *daf-19* mutants are strongly Daf-c across the normal temperature range for *C. elegans* (Table 1). They also recover very poorly from the dauer larval stage (data not shown).

The *daf-19* Daf-c phenotype likely results from morphological defects of sensory neurons: exposed amphid sensory neurons fail to fill with fluorescent dyes (Dyf phenotype) (Perkins et al., 1986; this work). Electron microscopy (EM) of one *daf-19* allele (*m86*) revealed that the ciliated endings of sensory neurons were entirely missing (Perkins et al., 1986). We confirmed this result with two additional *daf-19* alleles by using green fluorescent protein (GFP) fusions that are expressed in specific ciliated sensory neurons throughout development (Yu et al., 1997) (Figure 1 and Table 2). ASE is a chemosensory neuron in the head (Bargmann and Horvitz, 1991) with a cilium exposed to the environment. PQR is a tail neuron of unknown function that extends a cilium into the pseudocoelomic space. We found that *daf-19* mutants specifically lacked the cilium in both cell types (Figures 1D and 1E, lower panels). Cilia from wild-type animals and from mutants with structural defects in only the distal parts of the cilium were clearly distinguishable from *daf-19* (Figure 1D, top and middle panels). In addition, PQR dendrite length varied in *daf-19* (Figure 1E, lower panels). As a control, we examined a GFP fusion that is expressed specifically in AFD, a thermosensory neuron in the head (Mori and Ohshima, 1995) with a rudimentary cilium and many finger-like projections (microvilli). The finger-like microvilli at the end of the AFD dendrite were not visibly affected by *daf-19* and the other mutations tested (Figure 1C). Subcellular compartments other than the cilia in all of these neurons were relatively unaffected by *daf-19* (Table 2). As was reported for several other cilium structure–defective mutants (Peckol et al., 1999), we also occasionally found short extraneous processes emanating from or near the cell body in *daf-19* mutants (Table 2). As observed by EM and fluorescence (Perkins et al., 1986; this work), all of the large group of cilium structure–defective mutants except for *daf-19* retain sensory cilia to some extent. The unique severity of cilium defects in *daf-19* mutants suggests that *daf-19* is essential for sensory cilium formation.

daf-19 Encodes an RFX-Type Transcription Factor

We mapped *daf-19* to a small physical interval just right of *unc-4* on linkage group II. We cloned *daf-19* by transgenic rescue of *daf-19* (*m86*) and by sequencing of mutant alleles (Figure 2A). Three different *daf-19* cDNA clones, yk151d8, yk254c1, and yk457d6, were obtained from Yuji Kohara (*C. elegans* cDNA Sequencing Consortium). Since all the cDNA clones appeared incomplete at their 5′ ends, a full-length SL1 *trans*-spliced mRNA structure was determined by completing the two longest cDNA clones with RT-PCR and 5′ RACE. The two *daf-19* mRNAs encode predicted proteins of 780 or 805 amino acids, depending on the use of an alternatively spliced exon 4. The DAF-19 protein is a *C. elegans* member of the RFX-type transcription factor family (*Ce* RFX) (Emery et al., 1996a). Members of this family activate or repress the expression of diverse genes in humans, mice and yeasts. DAF-19 is the only member of this family in the *C. elegans* genome sequence, which is now essentially complete (*C. elegans* Sequencing Consortium, 1998). Multiple alignment of DAF-19 with its mammalian counterparts revealed a highly conserved DNA binding domain (DBD; Figures 2B and 2C) and dimerization domain (DIM; Figures 2B and 2D). Domains B and C, of unknown function (Figure 2B), are conserved to a lesser extent. DAF-19 is most similar to the RFX1–3 subgroup in mammals (Figures 2B–2D) (Emery et al., 1996a). No other similarities of significance were found between *daf-19* and other sequences in databases (December 1999).

daf-19 Is Expressed in Ciliated Sensory Neurons

To identify the cells in which *daf-19* is expressed, 2.9 kb of the *daf-19* promoter and about 10 kb of *daf-19* genomic sequence were used for a fusion of the GFP gene to *daf-19* just downstream of the DBD domain (Figure 2A). Expression was seen in a pattern of nuclei consistent with those of all ciliated sensory neurons (Figure 3) (White et al., 1986), in agreement with the cilium defects of *daf-19* mutants (Figure 1 and Table 2) (Perkins et al., 1986). We think this reporter correctly represents endogenous *daf-19* expression for two reasons. First, the fusion rescued the *daf-19* Daf-c and Dyf phenotypes, consistent with appropriate expression of a functional DAF-19 protein. This result suggests that DAF-19 can function in the absence of a DIM domain, as was shown for its close human homolog, *Hs* RFX1 (Reith et al., 1990). Second, GFP expression began around the 2-fold stage of embryogenesis, continued at high levels through the L1 and L2 larval stages, and then weakened or was absent (data not shown), consistent with a role in sensory cilium differentiation (Sulston et al., 1983; Fujiwara et al., 1999). In occasional animals that expressed GFP at higher levels than regularly observed, we noticed expression in a few additional neurons as well as hypodermal and intestinal cells. The significance of the expression in these cells is not clear.

RFX Target Sites Are Found in Promoters of Several Cilium Genes

The absence of sensory cilia in *daf-19* mutants, the *daf-19* expression pattern, the similarity of DAF-19 to RFX-type transcription factors, and the requirement of *daf-19* for the expression of *osm-6*, a gene implicated in cilium formation (Collet et al., 1998), together suggested that *daf-19* functions in the development of sensory cilia. We hypothesized that DAF-19 acts as a transcriptional activator of genes that function in ciliated sensory neurons (cilium genes).

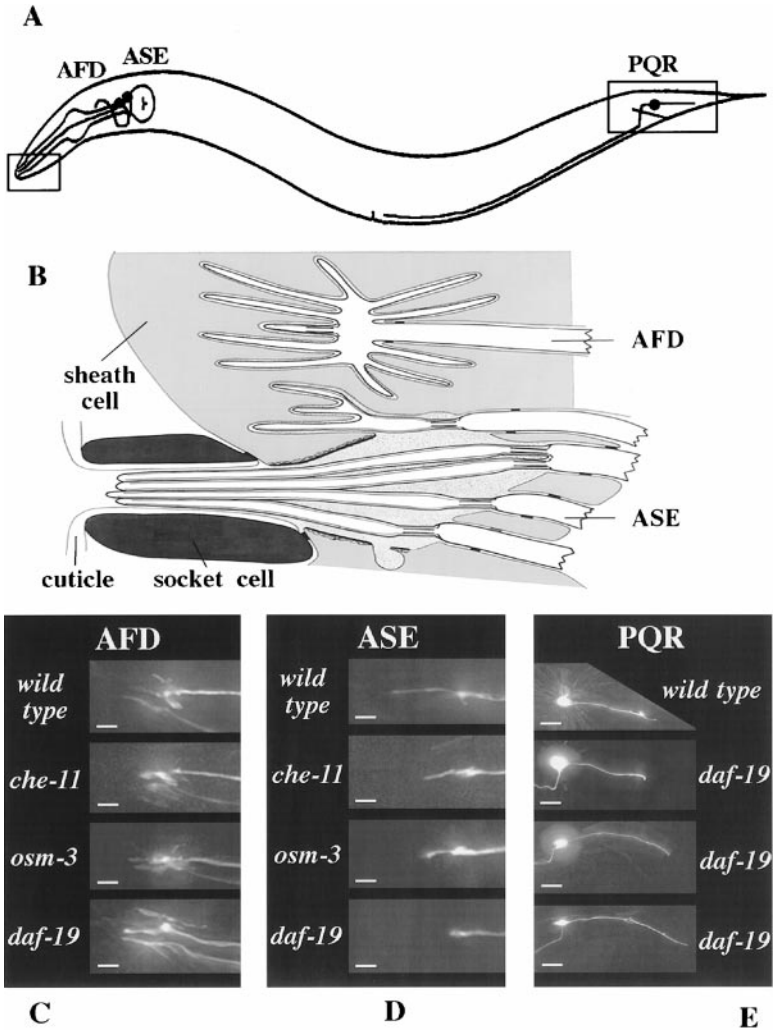

Figure 1. Cilia Defects of Sensory Neurons in *daf-19* Mutants

Transgenic animals harboring ciliated sensory neuron–specific GFP markers (*gcy-5/gcy-8/gcy-32::gfp*; Yu et al., 1997; cf. Table 2) were used to visualize cilia in the wild type and in cilium structure–defective mutants (*che-11, osm-3*, and *daf-19*). Anterior is to the left and dorsal is up. Bars represent 2 μm in (C) and (D) and 10 μm in (E).

(A) A schematic illustrating the positions of bipolar ciliated sensory neurons AFD, ASE, and PQR. For the bilateral pairs AFD and ASE of the amphid sensilla, only the left neurons are shown. Cell bodies are dots. The axons of AFD and ASE enter the nerve ring between the two pharyngeal bulbs. The axon of PQR enters the ventral nerve cord and follows an anteriorly directed trajectory. The dendrites extend anteriorly to the tip of the nose (AFD and ASE) or posteriorly (PQR) from the cell bodies. The sensory endings of all three neurons are positioned at the tip of the dendrites and are not distinguishable in this drawing. The rectangles depict the areas shown in (C)–(E).

(B) A schematic illustrating the sensory endings of some amphid sensory neurons (after Perkins et al., 1986). Dendritic tips are shown to the right. Sensory endings extend from these dendritic tips. The microvilli of AFD are encased within the amphid sheath cell. The cilium of ASE is exposed to the environment.

(C) The sensory endings (microvilli) of AFD in L1 larvae (foreground, AFDL; background, AFDR). Microvilli are clearly visible as finger-like projections at the tip of the dendrite (thick process to the right). AFD has only a rudimentary cilium, which is not visible here. Microvilli were indistinguishable between wild-type and mutant backgrounds throughout development.

(D) The sensory ending (cilium) of ASE in L1 larvae (GFP marker expression only in ASER). The cilium is visible as a thin projection at the tip of the dendrite (thick process to the right). The cilium is full length in wild type (top panel), reduced in length in mutants *che-11* and *osm*-3 (middle panels), and completely absent in *daf-19* mutants (bottom panel). Similar phenotypes were observed in each mutant throughout development.

(E) The sensory ending (cilium) of PQR in adults. The cell body is situated in the left part of each panel. The dendrite extends from the cell body posteriorly (thick process to the right). In wild type (top panel), a cilium is visible as a thin projection at the tip of the dendrite. In *daf-19* mutants (lower panels), the cilium is absent. Dendrites also grow to different lengths in *daf-19* mutants (lower panels). PQR anatomy was scored only at later larval (L3, L4) and adult stages, since this neuron is born at the mid L1 stage (White et al., 1986).

The promoter target sites (X boxes) of RFX-type transcription factors are known from in vitro binding studies and from work with mammalian cell culture and yeast (Reith et al., 1994; Emery et al., 1996b; Mach et al., 1996; Huang et al., 1998). The very high sequence identity in the DBD between DAF-19 and human RFX-type proteins suggested that DAF-19 might also act on X box sequences in *C. elegans*. We searched for matches to mammalian X boxes in promoter regions of more than 20 *C. elegans* genes that are expressed in ciliated sensory neurons (Experimental Procedures). We found sequences that matched well with RFX1 target sites within the promoters of *che-2*, *daf-19*, *osm-1*, and *osm-6* (Figure 4). In each case, key nucleotides for RFX binding were found to be conserved, and the match was located about 100 nt upstream from the predicted translational start site. These four genes are expressed in most or all ciliated sensory neurons (see below) and mutations in each of them cause all sensory cilia to be morphologically defective (Perkins et al., 1986). We did not find X box matches of similar significance in promoter regions of any genes that are expressed in only a subset of ciliated sensory neurons (Experimental Procedures), e.g., not in *gcy-5*, *gcy-8* and *gcy-32*. These genes are expressed independently of *daf-19* function (Figure 1). Our findings are consistent with *daf-19* being a transcriptional regulator of gene products that function broadly in sensory cilia.

daf-19 Regulates the Expression of X Box–Containing Cilium Genes

To test whether *daf-19* regulates the expression of cilium genes harboring X boxes in their promoters, we used an in vivo GFP expression assay. A DNA fragment containing about 2 kb of promoter through the translational

Table 2. Morphology of Three Sensory Neuron Classes

ASE (visualized with *gcy-5*::gfp)[a]				
Genotype	Cilium	Dendrite	Cell Body, Axon	Additional Process[b]
Wild Type	97 (full-length) 3 (shortened) 0 (absent)	100	100	2
daf-19 (m86)	0 (full-length) 16 (very short) 84 (absent)	100	100	35
daf-19 (sa190)	0 (full-length) 17 (very short) 83 (absent)	100	100	28
daf-19 (sa232)	0 (full-length) 9 (very short) 91 (absent)	100	100	32
osm-3 (e1806)	38 (full-length) 62 (shortened) 0 (absent)	100	100	6
che-11 (e1810)	32 (full-length) 68 (shortened) 0 (absent)	100	100	11
PQR (visualized with *gcy-32*::gfp)[a]				
Genotype	Cilium[c]	Dendrite	Cell Body, Axon	Additional Process[b]
Wild Type	78 (present) 19 (unclear) 3 (absent)	0 (short) 100 (normal) 0 (long)	100	9
daf-19 (m86)	6 (present) 45 (unclear) 49 (absent)	2 (short) 72 (normal) 26 (long)	100	29
daf-19 (sa190)	16 (present) 36 (unclear) 48 (absent)	9 (short) 64 (normal) 27 (long)	100	16
daf-19 (sa232)	4 (present) 38 (unclear) 58 (absent)	11 (short) 55 (normal) 34 (long)	100	17
AFD (visualized with *gcy-8*::gfp)[a]				
Genotype	Microvilli	Dendrite	Cell Body, Axon	Additional Process[b]
Wild Type	100	100	100	1
daf-19 (m86)	100	100	100	4
daf-19 (sa190)	100	100	100	1
daf-19 (sa232)	100	100	100	1
osm-3 (e1806)	100	100	100	3
che-11 (e1810)	100	100	100	3

[a] Data are percentages: the presence and morphological appearance of different subcellular compartments were observed by conventional fluorescence microscopy. Animals at the L1 or L2 larval stage were analyzed for ASE and AFD, two sensory neurons born during embryogenesis. L4 or adult animals were analyzed for PQR, a neuron born postembryonically. Between 55 and 85 animals were analyzed for each genotype.
[b] The class "additional process" describes mostly short extraneous processes emanating either from the cell body (all three sensory neurons), from axon bifurcations (ASE and AFD), or from dendrite bifurcations (PQR).
[c] If cilia appeared to be present in a *daf-19* background at the end of dendrites of PQR, they were frequently much shorter or grossly misshaped as compared to wild type.

start site of each gene was fused in frame to GFP-encoding DNA. We examined transgenic animals expressing each of these GFP fusions driven by promoters containing either a wild-type, mutated, or *C. elegans* consensus-derived X box sequence.

For *che-2*, *osm-1*, and *osm-6* (for *daf-19* see Experimental Procedures), wild-type promoters drove GFP expression in most or all ciliated sensory neurons throughout development after the 2-fold stage of embryogenesis (Table 3, first column; *osm-6*: cf. Figure 5A). These expression patterns were indistinguishable from those reported using mutant-rescuing GFP fusions for each of these genes (Collet et al., 1998; Fujiwara et al., 1999; J. Shaw, personal communication). In each case, promoters with mutated X boxes failed to express detectable GFP (Table 3, third column; *osm-6*: cf. Figure 5C). To confirm that the altered X box sequence was responsible for the loss of expression, we replaced the mutated X boxes with a *C. elegans* consensus-derived X box sequence (cf. Figure 4). In each case, this restored expression to near wild-type levels (Table 3, fourth column; *osm-6*: cf. Figure 5D). These experiments demonstrate

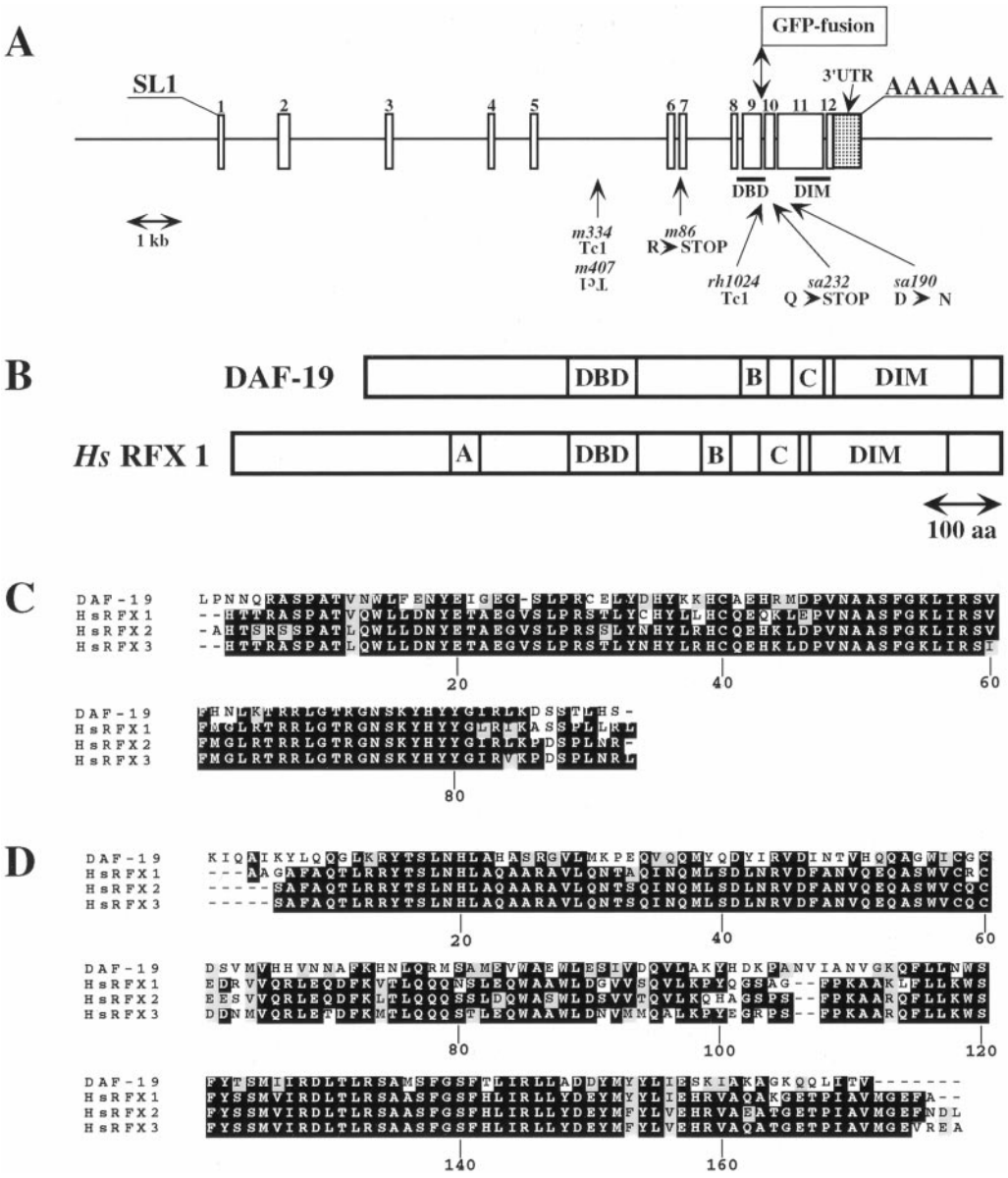

Figure 2. *daf-19* Encodes an RFX-Type Transcription Factor

(A) Genomic organization of the *daf-19* gene (F33H1.1). Numbered boxes depict exons. Exon 4 is alternatively spliced. The stippled box depicts the 3′ untranslated region of the *daf-19* message. *daf-19* is SL1 *trans*-spliced at the 5′ end. DBD means DNA binding domain; DIM means dimerization domain. The location of the translational fusion between *daf-19* and the GFP gene is indicated. There are six different *daf-19* mutant alleles. The reference allele, *m86*, affects cosmid F33H1-nt 9760 (C to T; resulting in a stop codon before all functionally conserved domains). Thus, *m86* is the most likely candidate for a molecular null allele. *sa190* affects F33H1-nt 7737 (G to A; changing a conserved Asp to Asn at the beginning of domain C). *sa232* affects F33H1-nt 8192 (C to T; resulting in a stop codon just after the DBD). *m334* and *m407* are both Tc1 insertions at F33H1-nt 11057/11058 (in opposite orientations in an intron). *rh1024* is a Tc1 insertion at F33H1-nt 8413/8414 (at the end of the DBD).

(B) Comparison of DAF-19 with one of its closest mammalian homologs, human *(Hs)* RFX1 (Emery et al., 1996a). Domains A, B, and C are defined only as blocks of sequence homology. They have no known function. DAF-19 does not have a domain A.

(C) Alignment of DBDs from DAF-19 and human RFX1–3. Identical amino acids are outlined in black, similar amino acids are outlined in gray.

(D) Alignment of DIMs from DAF-19 and human RFX1–3. Shading is as in (C).

that the X box is a key promoter element for the expression of a group of genes that function in the formation of all sensory cilia in *C. elegans*.

Moving wild-type and consensus-derived X box–containing transgenes into a *daf-19* background resulted in absent or drastically reduced GFP expression (Table 3, second and fifth columns; *osm-6*: cf. Figure 5B). Reduced expression manifested itself in fewer cells expressing GFP at much lower levels and at fewer developmental stages. This occasional low-level expression could mean that other factors might be involved in cilium gene regulation. Taken together, our data show that X box–promoted gene expression is *daf-19* dependent.

Based on these results we hypothesized that the tran-

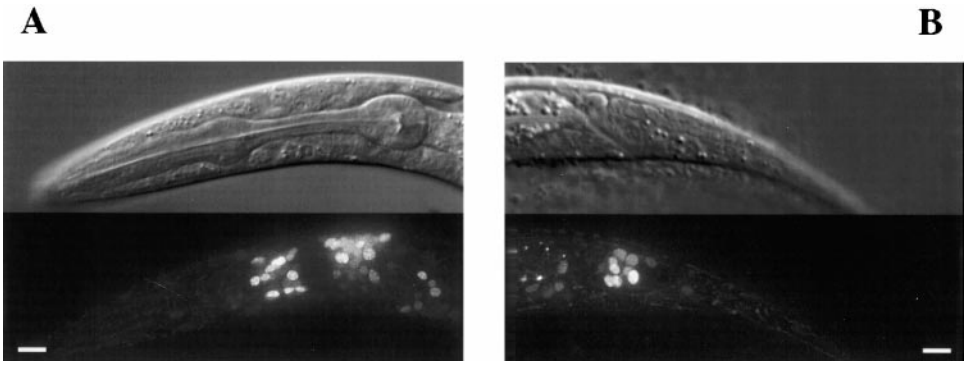

Figure 3. Expression of *daf-19::gfp* Fusion Genes

Nomarski (top panels) and fluorescence (bottom panels) images of *daf-19::gfp* transgenic animals at the L1 larval stage. The pattern of fluorescence is consistent with expression in all ciliated sensory neurons. Bars represent 5 μm. (A) Head. (B) Tail.

scription of genes functioning broadly in sensory cilia is dependent on DAF-19 and its target promoter element, the X box. This hypothesis predicts that novel genes that contain an appropriately positioned promoter X box sequence might also be expressed in most or all ciliated sensory neurons in a *daf-19*-dependent manner. In a genome-wide search for such genes, the strongest candidate was a novel gene, F02D8.3 (Figure 4). Using the in vivo GFP expression assay, this novel gene behaved exactly as predicted. In the wild-type background, F02D8.3::GFP was expressed in most or all ciliated sensory neurons in more than 90% of transgenic animals. In a *daf-19* mutant background, GFP expression was absent or drastically reduced: fewer than 5% of the animals expressed GFP. Thus, we were able to identify a ciliated sensory neuron gene based on the presence of an X box in its promoter. In summary, our results strongly support a model in which DAF-19 is the main transcriptional activator of a group of genes functioning in all sensory cilia.

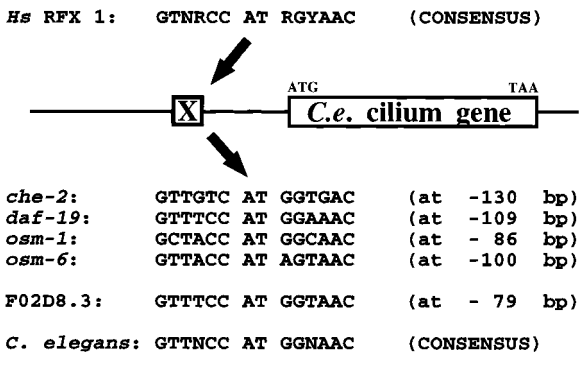

Figure 4. *C. elegans* Cilium Genes with Potential DAF-19 Target Sites in Their Promoters

Target sites for mammalian RFX-type transcription factors (X boxes) typically are 13–14 bp imperfect inverted repeats. Mammalian X boxes (the *Hs* RFX1 target site consensus is shown) served as queries for a search for *C. elegans* X boxes (Experimental Procedures). Lines depict 5′ and 3′ untranslated regions. The open box marked with an X depicts putative *C. elegans* X boxes. The open box depicts the coding region. Distances given after the *C. elegans* X box sequences are upstream of the translation start site (ATG) of the respective gene.

Discussion

We have shown that *daf-19* encodes the single *C. elegans* member of the RFX-type transcription factor family. *daf-19* is expressed in differentiating ciliated sensory neurons and *daf-19* mutants lack sensory cilia, resulting in severe sensory defects. DAF-19 target sites (X boxes) are present in promoters of several genes that are broadly expressed in ciliated sensory neurons, but not in promoters of genes with a more restricted expression pattern within this class of neurons. Using an in vivo assay, we showed that expression of the X box–containing genes was dependent on both *daf-19* function and the presence of the promoter X box. These results demonstrate that *daf-19* has a critical function in the development of ciliated sensory neurons, and support a model in which *daf-19* expression specifies the formation of a sensory cilium, thereby enabling these neurons to receive signals from the environment.

daf-19 Affects Sensory Cilium Development

A variety of studies of neuronal development indicate that the progressive restriction of developmental potential within neuronal cell lineages is achieved through interactions between extrinsic and intrinsic factors. A current model is that the competence of neuronal precursors to respond to given cues is defined in part by the expression of a temporally changing set of transcription factors (Pfaff and Kintner, 1998; Zipursky and Rubin, 1994), as shown, for example, for the differentiation of touch sensory neurons in *C. elegans* (Ruvkun, 1997; Duggan et al., 1998). Our results suggest that *daf-19* acts late in the cascade of events required for ciliated sensory neuron development, after cell fate has been firmly established. Mutations in *daf-19* do not cause cell fate transformations but interfere with a specific function late in ciliated sensory neuron differentiation.

In contrast to their effects on sensory cilia (Perkins et al., 1986; this work), *daf-19* mutations have relatively little effect on other aspects of the morphology of the three analyzed ciliated sensory neurons (AFD, ASE, and PQR). Specifically, cell bodies were present and positioned correctly and dendritic and axonal trajectories were grossly normal (but see below). These results suggest that most aspects of early cell fate are normal in

Table 3. Expression Analyses Using an In Vivo GFP Expression Assay[a]

Type of X box	Wild Type		Mutated	*C. elegans* Consensus-Derived	
Genotype	Wild Type	*daf-19*	Wild Type	Wild Type	*daf-19*
che-2::gfp	50	ND[b]	0	74	0
	72	0	0	0	ND
	65	0	0	6	0
osm-1::gfp	100	21	0	98	9
	100	37	0	96	5
	99	ND	0	97	ND
osm-6::gfp	100	4	0	50	6
	100	ND	0	96	ND
	98	0	0	98	5
Strength of Expression	very strong to strong	very weak to absent	absent	strong to moderate	very weak to absent

[a] Data are given as percent expression in ciliated sensory neurons in the head of adult animals. The three genes tested are expressed in most of the 60 ciliated sensory neurons of the animal. Three independent transgenic lines were analyzed for each gene. Each number represents the data for one transgenic line. For transgenic lines containing wild-type X box sequences and transgenic lines containing *C. elegans* consensus-derived X box sequences, the transgene was also moved from the wild type into a *daf-19* background. More than 100 animals were analyzed for each transgenic line.
[b] Abbreviation: ND, experiment not done.

daf-19 mutants, including the migration that leads to correct placement of their cell bodies and most aspects of dendrite and axon pathfinding. The specificity of the *daf-19* ciliary defects is further supported by the fact that another sensory specialization, the finger-like microvilli of AFD, were unaffected in *daf-19* mutants. Moreover, *gcy-5*, *gcy-8*, and *gcy-32*, which encode guanylyl cyclases implicated in sensory signal transduction (Mori and Ohshima, 1997; Yu et al., 1997; Prasad and Reed, 1999), were still expressed in the absence of *daf-19* function.

We were able to observe ASE and PQR throughout development. At the developmental stage that cilia first became visible in the wild type, cilia were never visible in *daf-19* mutants, supporting the idea that their defect is in cilium formation, rather than having a degenerative effect on cilia. Consistent with this notion, we observed *daf-19::gfp* expression primarily during the second half of embryogenesis, the major time period when cilia are generated (Fujiwara et al., 1999).

We noted two abnormalities other than cilia defects in *daf-19* mutants. First, dendrite length varied in PQR but not in ASE. The different migration patterns of these two neurons might offer an explanation. During embryonic development the ASE cell body forms a rudimentary sensillum at the tip of the head, then migrates posteriorly, leaving its dendrite behind (Sulston et al., 1983). In contrast, during postembryonic development, the stationary PQR cell body extends a dendrite posteriorly (Sulston and Horvitz, 1977) in a process analogous to axonal outgrowth. We suggest that in PQR the termination of this outgrowth is coordinated with cilium formation. Second, we observed occasional short extraneous processes, in particular in ASE and PQR, in addition to normal dendrites and axons. Mutations in a diverse set of genes, including cilium structure genes, have been shown to cause very similar phenotypes (Coburn and Bargmann, 1996; Hobert et al., 1997; Coburn et al., 1998; Peckol et al., 1999), suggesting that these low penetrance abnormalities are not *daf-19* specific.

daf-19 Regulates Only Certain Cilium Genes

In *C. elegans*, many genes are expressed in ciliated sensory neurons and are implicated in functioning in their cilia: (1) genes involved in signal reception (e.g., chemosensory receptors) (Troemel et al., 1995; Sengupta et al., 1996) and in signal transduction (Mori and Ohshima, 1997; Prasad and Reed, 1999), (2) genes implicated in targeting or transporting molecules to the cilia (Tabish et al., 1995; Dwyer et al., 1998; Signor et al., 1999b), and (3) genes involved in the structure of cilia (Perkins et al., 1986; Starich et al., 1995; Collet et al., 1998; Roayaie et al., 1998). The transcriptional regulation of most of these genes is not understood. We searched for X boxes in promoters of a representative subset of these genes (Experimental Procedures). We found significant matches to X box target sites of mammalian RFX1 (Reith et al., 1994; Emery et al., 1996b) in promoters of only one group of cilium genes: *che-2*, *daf-19*, *osm-1*, and *osm-6*. Based on EM observations, these four genes have long been grouped together because mutations in them cause structural defects in all sensory cilia (Lewis and Hodgkin, 1977; Perkins et al., 1986). *che-3*, another member of this group of genes (Lewis and Hodgkin, 1977; Perkins et al., 1986; Wicks et al., 2000), does not have a promoter X box. The last two members of this group, *che-13* and *osm-5*, have not yet been cloned. Expression of *che-2*, *daf-19*, *osm-1*, and *osm-6* was detected in ciliated sensory neurons at times consistent with these genes functioning in cilium morphogenesis and architecture (Collet et al., 1998; Fujiwara et al., 1999; J. Shaw, personal communication; this work). In addition, we demonstrated that *che-2*, *osm-1*, and *osm-6* expression was *daf-19* and X box dependent. The molecular identities of these genes are intriguing. *che-2* encodes a novel WD40-repeat protein thought to be involved in protein–protein interactions in the assembly of large multiprotein complexes (Fujiwara et al., 1999). *osm-1* and *osm-6* encode proteins related to p172 and p52, respectively, which are involved in intraflagellar

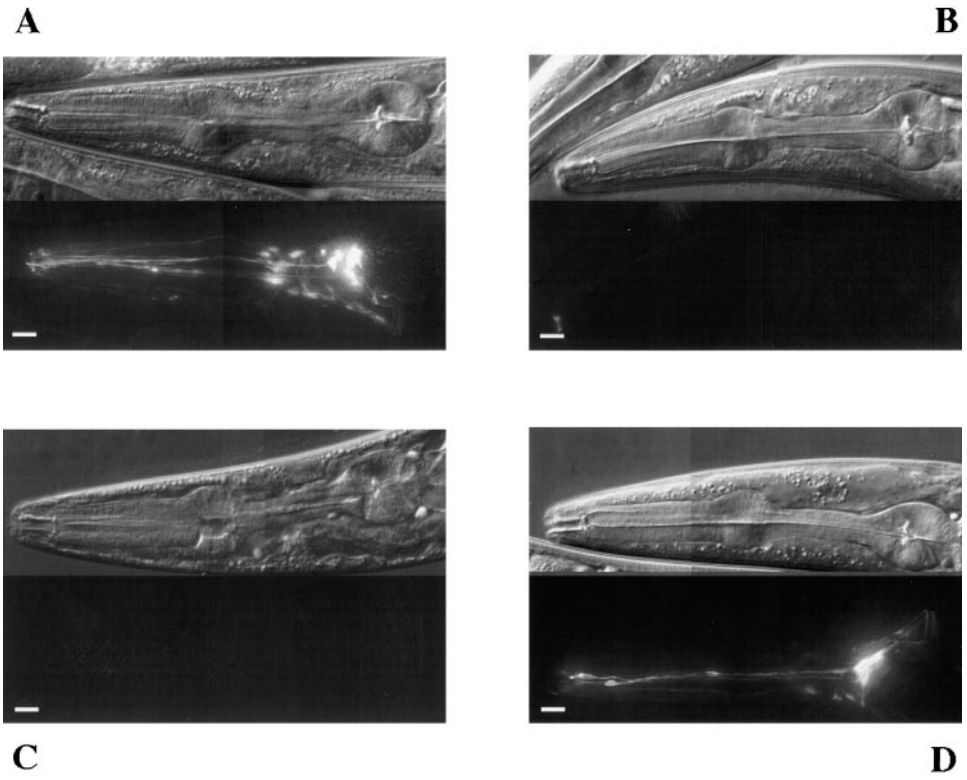

Figure 5. Expression from *osm-6::gfp* Promoter Fusions

Nomarski (top panels) and fluorescence (bottom panels) images of the heads of *osm-6::gfp* transgenic adults (cf. Table 3). Anterior is to the left and dorsal is up. Bars represent 10 μm.

(A) The wild-type *osm-6* promoter drives expression of the *osm-6::gfp* transgene in the wild type. GFP expression is visible in ciliated sensory neurons.

(B) The same transgene shown in (A) when in a *daf-19* mutant background. GFP expression is absent or severely reduced.

(C) An *osm-6* promoter containing a mutated X box fails to drive GFP expression in the wild type. GFP expression is absent.

(D) The *osm-6* promoter shown in (C) with a *C. elegans* consensus derived X box sequence reintroduced partially restores GFP expression in the wild type. GFP expression is visible in ciliated sensory neurons.

transport, a process required for the assembly and function of motile flagella in the unicellular green alga *Chlamydomonas* (Cole et al., 1998; Rosenbaum et al., 1999; J. Shaw, personal communication). Consistent with these identities, *osm-1::gfp* and *osm-6::gfp* fluorescent dots were observed to move within sensory cilia (Orozco et al., 1999; Signor et al., 1999a). The mammalian homolog of *osm-6* is of neuronal origin but has no known function (Collet et al., 1998).

Several other genes are involved in the specialized architecture of some sensory cilia but not others, for example *osm-3* (Perkins et al., 1986; Tabish et al., 1995) and *odr-3* (Bargmann et al., 1993; Roayaie et al., 1998), or are involved in neuron-specific signal reception and transduction (Mori and Ohshima, 1997; Prasad and Reed, 1999), for example the *gcy-5*, *gcy-8* and *gcy-32* signal transducers (Yu et al., 1997) used as cell-specific markers in our study. These genes do not require DAF-19 for their transcription (cf. Figure 1) and their promoters lack X boxes (Experimental Procedures).

We propose a model in which DAF-19 is a key transcriptional regulator of genes expressed broadly in most or all sensory cilia. In parallel or subsequently, other factors drive the expression of cell-specific cilium structure elements, signal receptors, and signal transducers. These cell-specific factors specify the diversity of structure and function of ciliated sensory neurons, while *daf-19* specifies their commonalities.

At present we are using the *C. elegans* X box consensus sequence to search through the entire *C. elegans* genome sequence (*C. elegans* Sequencing Consortium, 1998) to find novel members of the group of DAF-19 regulated genes. The first candidate gene identified with this method, F02D8.3, a homolog of a mammalian brain protein of unknown function, was expressed specifically in ciliated sensory neurons in a *daf-19*-dependent manner. Thus, such a search strategy offers the potential to identify many more of the proposed protein components of sensory cilia (Orozco et al., 1999; Rosenbaum et al., 1999).

The Mammalian Homologs of DAF-19

DAF-19 is most homologous to the mammalian RFX1–3 subgroup of RFX-type transcription factors, and X boxes for DAF-19 are more similar to X boxes for RFX1 than to X boxes for RFX5 (Reith et al., 1994; Emery et al., 1996a, 1996b; Mach et al., 1996). Very little is known about possible cellular functions of the RFX1–3 subgroup, in particular about its target genes (Reinhold et al., 1995; Iwama et al., 1999). RFX1 is expressed in many different tissues, RFX2 predominantly in the testis, and

RFX3 predominantly in brain tissues (Reith et al., 1994). It is tempting to speculate that the mammalian proteins serve analogous functions to DAF-19 in these tissues. RFX2, for example, could be involved in differentiating flagella in sperm cells. The regulation of cilia and flagella differentiation might be preserved from nematodes to mammals.

Experimental Procedures

Strains and Assays

General growth conditions for *C. elegans* strains were as described (Brenner, 1974). Strains were grown at 20°C unless stated otherwise. The wild-type strain was N2 Bristol. The following mutations were used: LG (linkage group) II: *dpy-10 (e128), rol-6 (e187), unc-4 (e120), egl-43 (n997), unc-53 (e404), bli-1 (e769), unc-52 (e444);* LG IV: *osm-3 (e1806);* LG V: *che-11 (e1810), osm-6 (p811);* LG X: *che-2 (e1033), lin-15 (n765), osm-1 (p808).* The following extrachromosomal arrays were used: *adEx1262 (gcy-5::gfp), adEx1268 (gcy-8::gfp)* and *adEx1295 (gcy-32::gfp)* were employed as cell-specific markers (Yu et al., 1997). *saEx310–314* were assessed for *daf-19* transgenic rescue. *saEx488–490* were used for *daf-19::gfp* expression experiments. *saEx470–487* and *saEx523* were used for *che-2/osm-1/osm-6/F02D8.3::gfp* expression experiments. All strains used and strain construction details are available on request. Dauer formation assays and fluorescent dye (FITC) filling assays were performed essentially as described (Perkins et al., 1986; Malone and Thomas, 1994).

Isolation of Alleles, Genetic Mapping, Cloning, and Molecular Characterization of *daf-19*

EMS generated alleles: *m86* (reference allele) and *sa190* were isolated in screens for Daf-c mutations (Malone and Thomas, 1994; D. Riddle, personal communication). *sa232* was isolated in a Daf-c noncomplementation screen against *m86*. Briefly, hermaphrodites of the strain JT6373 (*rol-6 [e187] daf-19 [m86] unc-53 [e404]*) were crossed to N2 males mutagenized with EMS and the progeny were screened for non-Rol, non-Unc dauers. Tc1-transposon/mutator alleles: *m334* and *m407* were isolated in screens for Daf-c mutations (D. Riddle, personal communication). *rh1024* was isolated by E. Hedgecock and shown to be an allele of *daf-19* by D. Riddle. All alleles failed to complement the *daf-19 (m86)* Daf-c phenotype and FITC dye filling defect (Dyf phenotype). All *daf-19* mutations are recessive reduction-of-function alleles. *daf-19* was previously mapped to the vicinity of *unc-4* on LG II (Perkins et al., 1986). Fine mapping with deficiencies and 3-factor crosses using alleles of *unc-4, egl-43,* and *bli-1* followed standard procedures: (1) *unc-4* (4/18 recombinants) *daf-19* (14/18) *bli-1*; (2) *unc-4* (10/41) *egl-43* (31/41) *daf-19*. Cosmids and cosmid subclones were tested for transgenic rescue of the Daf-c and Dyf phenotypes of *daf-19 (m86).* Germline transformation: DNA injections into the strain JT8651 (*daf-19[m86]/mnC1; lin-15[n765]*) were performed by standard methods (Mello et al., 1991) using *lin-15* (+) at 60 ng/μl as cotransformation marker DNA (Huang et al., 1994) and test DNA at various concentrations. Stable transgenic lines were obtained from individual F1 progeny that were rescued for the *lin-15* Muv phenotype. All six available mutations in *daf-19* were sequenced on both strands directly from purified bulk PCR products. For the EMS generated alleles, all exons, neighboring intron sequences, and the entire 5′ and 3′ UTR's were sequenced. Tc1 insertion alleles were mapped by generating *daf-19*/Tc1 specific junction PCR products before sequencing.

General Molecular Biology Methods

Manipulations were performed according to standard procedures (Sambrook et al., 1989). Cloned worm DNA, total worm DNA, or single worms were used for PCR amplifications for direct sequencing or for subcloning (Sambrook et al., 1989). Clones, primer sequences, and PCR conditions are available on request. An ABI Prism kit (Perkin Elmer) was used for DNA sequencing. Sequencing gels were run at the UW Biochemistry sequencing facility (ABI Prism sequencer; Perkin Elmer).

DNA Sequence Analyses

All *C. elegans* genome sequence information used for this study was obtained directly from the *C. elegans* Genome Sequencing Centers (http://www.sanger.ac.uk/Projects/C_elegans/ and http://genome.wustl.edu/gsc/C_elegans) (*C. elegans* Sequencing Consortium, 1998). Except for *che-11*, *daf-10*, and *osm-1* (S. Stone, A. Davies, J. Shaw, personal communication), gene identities were extracted from the *C. elegans* database ACeDB or references therein (http://elegans.swmed.edu/genome.shtml#ACEDB). We used BLAST 2.0 (http://www.ncbi.nlm.nih.gov/BLAST/) (Altschul et al., 1997) to identify and evaluate homologs of DAF-19. We used the ClustalW 1.7 sequence alignment tool (http://dot.imgen.bcm.tmc.edu:9331/index.html) (Thompson et al., 1994) and Boxshade 3.21 (http://www.ch.embnet.org/software/BOX_form.html) to align and display the DBD and DIM of DAF-19 and its closest mammalian homologs, RFX1–3.

For the X box search we used ClustalW 1.7. Six mammalian X box sequences served as queries: HLA-DRA, EF-C consensus, HBV (all from Reith et al., 1994), HBV-NRE gamma (Buckwold et al., 1997), MIF-1 (Reinhold et al., 1995), and RFX1 consensus (Emery et al., 1996b). We searched through a representative subset (more than twenty genomic sequence stretches encompassing ±3 kb from the presumed ATGs) of (1) genes implicated in signal reception and transduction in ciliated sensory neurons: *daf-11* (B0240.3), *daf-21* (C47E8.5), *egl-2* (F16B3.1), *gcy-5* (ZK970.6), *gcy-8* (C49H3.2), *gcy-32* (C06B3.8), *odr-3* (C34D1.3), *odr-10* (C53B7.5), *osm-9* (B0212.5), *srb-6* (R05H5.6), and *str-1* (C42D4.5); (2) genes expected or known to function in all ciliated sensory neurons: *che-2* (F38G1.1), *che-3* (F18C12.1), *daf-19* (F33H1.1), *osm-1* (T27B1.1), and *osm-6* (R31.3); and (3) genes expected or known to function in subsets of the ciliated sensory neuron class: *ceh-23* (ZK652.5), *che-11* (C27A7.4), *daf-10* (F23B2.4), *odr-4* (Y102E9.1), *odr-7* (T18D3.2), *osm-3* (M02B7.3), and *tub-1* (F10B5.4). The following genes served as negative controls as they were shown not to be expressed or not to function in ciliated sensory neurons: *egl-38* (C04G2.7), *nrf-6* (C08B11.4), and *unc-54* (F11C3.3). Because X boxes are fairly short, matches of low significance between query and subject sequences were always observed. Our search results were nonexhaustive because matches were accepted as highly significant only when (1) the match was at a distance of around 100 nt upstream of the ATG, (2) several of the RFX1–3 type X box query sequences were matched and, (3) conserved nucleotide positions within the X box matched. Only sequences in the promoters of *che-2, daf-19, osm-1*, and *osm-6* fulfilled these criteria. In the promoter region of *odr-4*, a match of lower significance was found at a site further upstream of the ATG than was the case for the other genes (P. S., unpublished data).

Generation and Analyses of Expression Constructs

Promoter regions (about 2 kb long) of *che-2, daf-19, osm-1, osm-6*, and F02D8.3 were amplified from cloned worm DNA by PCR. The primers contained restriction enzyme sites for ligation into the GFP vector pPD95.77. The promoters were fused in-frame to GFP within the first ten codons of the gene in question. Wild-type X boxes within promoters were mutated by overlapping PCR primed mutagenesis, replacing the X box with nonspecific nucleotides containing an indicative restriction enzyme site (NgoM IV; CGCGGC CG GCCGCG). Mutated X boxes were replaced by cutting with NgoMIV and cloning in oligonucleotides containing *C. elegans* consensus-derived X box sequences (GTTACC AT GGTAAC). The consensus-derived X box differed from the respective wild-type X boxes by one to three nucleotides. As verified by sequencing, plasmid junctions were correct and the proximal 500–600 bp to the start codon of the respective promoter GFP fusions were identical to wild type except for the intended sequence changes. The promoter GFP fusions were introduced into worms by germline transformation typically at 100 ng/μl. The injected strain JT8651 (*daf-19[m86]/mnC1; lin-15[n765]*) served as wild-type background, since *daf-19 (m86)* is fully recessive. Segregating dauers were recovered at 15°C to obtain a *daf-19* homozygous background. GFP expression was analyzed in stable extrachromosomal transgenic lines at 1000× magnification (Zeiss Axioskop) by conventional fluorescence microscopy. Representative cohorts of animals of each genotype and transgenic line were examined at most developmental stages between the embryo and

adult stage. Quantitative data (Table 3) were obtained at the highest magnification on a standard stereo dissecting microscope (Wild Mikroskope) with a fluorescent light attachment (Kramer Scientific) only for the adult stage since the transformation marker *lin-15* permits unambiguous detection of transgenesis only at this stage. Examinations were performed blind, except when *daf-19* mutants were looked at, since the presence of dauers on the plates made blind scoring impossible. For comparisons, the relevant genotypes and X box construct transgenes were analyzed side by side.

We were not able to successfully demonstrate *daf-19::gfp* expression by translationally inserting the GFP gene into a full-length *daf-19* genomic clone after the DIM, or by replacing DBD and DIM, or by translationally fusing the GFP gene to *daf-19* within the first or second exon (*daf-19* promoter length in all cases was 2.9 kb). We did achieve successful *daf-19::gfp* expression only when a GFP cassette (coding region and *unc-54* 3′UTR; from GFP vector pPD95.77) was inserted into a full-length *daf-19* genomic clone (promoter length was 2.9 kb) just after the DBD into the PstI-site (within exon 9; GFP thus replaced *daf-19* DIM and 3′UTR). Since this translational fusion rescued *daf-19*-specific phenotypes, the in vivo X box analyses described above were not possible. *daf-19::gfp* expression in identified neurons was analyzed at 1000× magnification (Zeiss Axioskop) by Nomarski and conventional fluorescence microscopy. Neuronal cell anatomies and identities followed published descriptions (Ward et al., 1975; Ware et al., 1975; Sulston and Horvitz, 1977; Sulston et al., 1983; White et al., 1986; Hall and Russell, 1991).

High-Resolution Microscopy

For precise imaging of GFP fluorescence in subcellular compartments (Figures 1, 3, and 5), a Deltavision microscope setup (Silicon Graphics) was used. Worms were put into 0.5 μl M9 buffer on a very thin 2% agarose pad containing an anesthetic, and were observed with an inverted microscope (Zeiss Axiovert) at a 63× objective magnification (NA = 1.40). This setup was equipped with a multiwavelength CCD camera (Quantix) and the stage and all shutters and filters were computer driven (Applied Precision). 3D data stacks were acquired in the FITC channel by moving the focal plane in 0.4 μm increments through the entire worm. Background and out-of-focus signal were removed using a conservative, reiterative (15x) deconvolution algorithm (Agard et al., 1989; Scalettar et al., 1996). 3D data stacks were combined using maximum intensity projections of all data points along the z axis.

Acknowledgments

We thank the following people for technical assistance, helpful discussions, unpublished information, *C. elegans* strains, cosmid clones, cDNA clones and GFP vectors: L. Avery, A. Coulson, B. Durand, A. Fire, D. Garbers, T. Holzman, I. Katsura, Y. Kohara, J. Miller, W. Reith, D. Riddle, J. Shaw, S. Tat, S. Wicks, and especially members of our laboratory. We thank M. Ailion, R. Choy, T. Inoue, L. Newton, J. Scholey, and J. Shaw for critical reading of the manuscript. We thank the *C. elegans* Genome Sequencing Consortium for providing genome sequence information and the *Caenorhabditis* Genetics Center, which is funded by the National Institutes of Health, for providing some of the *C. elegans* strains used in this study. This work was supported by a Public Health Service Grant to J. H. T. (R01 GM48700). P. S. was supported by postdoctoral fellowships from the Erwin Schrödinger Foundation (Vienna, Austria) and from the Human Frontier Science Promotion Organization (Strasbourg, France).

Received November 11, 1999; revised December 27, 1999.

References

Agard, D.A., Hiraoka, Y., Shaw, P., and Sedat, J.W. (1989). Fluorescence microscopy in three dimensions. Methods Cell Biol. *30*, 353–377.

Altschul, S.F., Madden, T.L., Schaffer, A.A., Zhang, J., Zhang, Z., Miller, W., and Lipman, D.J. (1997). Gapped BLAST and PSI-BLAST: a new generation of protein database search programs. Nucleic Acids Res. *25*, 3389–3402.

Bargmann, C.I., and Horvitz, H.R. (1991). Chemosensory neurons with overlapping functions direct chemotaxis to multiple chemicals in *C. elegans*. Neuron *7*, 729–742.

Bargmann, C.I., and Mori, I. (1997). Chemotaxis and thermotaxis. In *C. elegans* II, D.L. Riddle, T. Blumenthal, B.J. Meyer, and J.R. Priess, eds. (Cold Spring Harbor, NY: Cold Spring Harbor Laboratory Press), pp. 717–737.

Bargmann, C.I., Hartwieg, E., and Horvitz, H.R. (1993). Odorant-selective genes and neurons mediate olfaction in *C. elegans*. Cell *74*, 515–527.

Brenner, S. (1974). The genetics of *Caenorhabditis elegans*. Genetics *77*, 71–94.

Buckwold, V.E., Chen, M., and Ou, J.H. (1997). Interaction of transcription factors RFX1 and MIBP1 with the gamma motif of the negative regulatory element of the hepatitis B virus core promoter. Virology *227*, 515–518.

Coburn, C.M., and Bargmann, C.I. (1996). A putative cyclic nucleotide-gated channel is required for sensory development and function in *C. elegans*. Neuron *17*, 695–706.

Coburn, C.M., Mori, I., Ohshima, Y., and Bargmann, C.I. (1998). A cyclic nucleotide-gated channel inhibits sensory axon outgrowth in larval and adult *Caenorhabditis elegans*: a distinct pathway for maintenance of sensory axon structure. Development *125*, 249–258.

Cole, D.G., Diener, D.R., Himelblau, A.L., Beech, P.L., Fuster, J.C., and Rosenbaum, J.L. (1998). *Chlamydomonas* kinesin-II-dependent intraflagellar transport (IFT): IFT particles contain proteins required for ciliary assembly in *Caenorhabditis elegans* sensory neurons. J. Cell Biol. *141*, 993–1008.

Collet, J., Spike, C.A., Lundquist, E.A., Shaw, J.E., and Herman, R.K. (1998). Analysis of *osm-6*, a gene that affects sensory cilium structure and sensory neuron function in *Caenorhabditis elegans*. Genetics *148*, 187–200.

C. elegans Sequencing Consortium (1998). Genome sequence of the nematode *C. elegans*: a platform for investigating biology. Science *282*, 2012–2018.

Driscoll, M., and Kaplan, J. (1997). Mechanotransduction. In *C. elegans* II, D.L. Riddle, T. Blumenthal, B.J. Meyer, and J. R. Priess, eds. (Cold Spring Harbor, NY: Cold Spring Harbor Laboratory Press), pp. 645–677.

Duggan, A., Ma, C., and Chalfie, M. (1998). Regulation of touch receptor differentiation by the *Caenorhabditis elegans mec-3* and *unc-86* genes. Development *125*, 4107–4119.

Dutcher, S.K. (1995). Flagellar assembly in two hundred and fifty easy-to-follow steps. Trends Genet. *11*, 398–404.

Dwyer, N.D., Troemel, E.R., Sengupta, P., and Bargmann, C.I. (1998). Odorant receptor localization to olfactory cilia is mediated by ODR-4, a novel membrane-associated protein. Cell *93*, 455–466.

Emery, P., Durand, B., Mach, B., and Reith, W. (1996a). RFX proteins, a novel family of DNA binding proteins conserved in the eukaryotic kingdom. Nucleic Acids Res. *24*, 803–807.

Emery, P., Strubin, M., Hofmann, K., Bucher, P., Mach, B., and Reith, W. (1996b). A consensus motif in the RFX DNA binding domain and binding domain mutants with altered specificity. Mol. Cell Biol. *16*, 4486–4494.

Fujiwara, M., Ishihara, T., and Katsura, I. (1999). A novel WD40 protein, CHE-2, acts cell-autonomously in the formation of *C. elegans* sensory cilia. Development *126*, 4839–4848.

Hall, D.H., and Russell, R.L. (1991). The posterior nervous system of the nematode *Caenorhabditis elegans*: serial reconstruction of identified neurons and complete pattern of synaptic interactions. J. Neurosci. *11*, 1–22.

Hobert, O., Mori, I., Yamashita, Y., Honda, H., Ohshima, Y., Liu, Y., and Ruvkun, G. (1997). Regulation of interneuron function in the *C. elegans* thermoregulatory pathway by the *ttx-3* LIM homeobox gene. Neuron *19*, 345–357.

Huang, L.S., Tzou, P., and Sternberg, P.W. (1994). The *lin-15* locus encodes two negative regulators of *Caenorhabditis elegans* vulval development. Mol. Biol. Cell *5*, 395–411.

Huang, M., Zhou, Z., and Elledge, S.J. (1998). The DNA replication and damage checkpoint pathways induce transcription by inhibition of the Crt1 repressor. Cell *94*, 595–605.

Iwama, A., Pan, J., Zhang, P., Reith, W., Mach, B., Tenen, D.G., and Sun, Z. (1999). Dimeric RFX proteins contribute to the activity and

lineage specificity of the interleukin-5 receptor alpha promoter through activation and repression domains. Mol. Cell Biol. *19*, 3940–3950.

Johnson, K.A. (1995). Keeping the beat: form meets function in the *Chlamydomonas* flagellum. BioEssays *17*, 847–854.

Kaplan, J.M., and Horvitz, H.R. (1993). A dual mechanosensory and chemosensory neuron in *Caenorhabditis elegans*. Proc. Natl. Acad. Sci. USA *90*, 2227–2231.

Lewis, J.A., and Hodgkin, J.A. (1977). Specific neuroanatomical changes in chemosensory mutants of the nematode *Caenorhabditis elegans*. J. Comp. Neurol. *172*, 489–510.

Mach, B., Steimle, V., Martinez-Soria, E., and Reith, W. (1996). Regulation of MHC class II genes: lessons from a disease. Annu. Rev. Immunol. *14*, 301–331.

Malone, E.A., and Thomas, J.H. (1994). A screen for nonconditional dauer-constitutive mutations in *Caenorhabditis elegans*. Genetics *136*, 879–886.

Mello, C.C., Kramer, J.M., Stinchcomb, D., and Ambros, V. (1991). Efficient gene transfer in *C. elegans*: extrachromosomal maintenance and integration of transforming sequences. EMBO J. *10*, 3959–3970.

Mori, I., and Ohshima, Y. (1995). Neural regulation of thermotaxis in *Caenorhabditis elegans*. Nature *376*, 344–348.

Mori, I., and Ohshima, Y. (1997). Molecular neurogenetics of chemotaxis and thermotaxis in the nematode *Caenorhabditis elegans*. Bioessays *19*, 1055–1064.

Orozco, J.T., Wedaman, K.P., Signor, D., Brown, H., Rose, L., and Scholey, J.M. (1999). Movement of motor and cargo along cilia. Nature *398*, 674.

Peckol, E.L., Zallen, J.A., Yarrow, J.C., and Bargmann, C.I. (1999). Sensory activity affects sensory axon development in *C. elegans*. Development *126*, 1891–1902.

Perkins, L.A., Hedgecock, E.M., Thomson, J.N., and Culotti, J.G. (1986). Mutant sensory cilia in the nematode *Caenorhabditis elegans*. Dev. Biol. *117*, 456–487.

Pfaff, S., and Kintner, C. (1998). Neuronal diversification: development of motor neuron subtypes. Curr. Opin. Neurobiol. *8*, 27–36.

Prasad, B.C., and Reed, R.R. (1999). Chemosensation: molecular mechanisms in worms and mammals. Trends Genet. *15*, 150–153.

Reinhold, W., Emens, L., Itkes, A., Blake, M., Ichinose, I., and Zajac-Kaye, M. (1995). The myc intron-binding polypeptide associates with RFX1 in vivo and binds to the major histocompatibility complex class II promoter region, to the hepatitis B virus enhancer, and to regulatory regions of several distinct viral genes. Mol. Cell Biol. *15*, 3041–3048.

Reith, W., Herrero-Sanchez, C., Kobr, M., Silacci, P., Berte, C., Barras, E., Fey, S., and Mach, B. (1990). MHC class II regulatory factor RFX has a novel DNA-binding domain and a functionally independent dimerization domain. Genes Dev. *4*, 1528–1540.

Reith, W., Ucla, C., Barras, E., Gaud, A., Durand, B., Herrero-Sanchez, C., Kobr, M., and Mach, B. (1994). RFX1, a transactivator of hepatitis B virus enhancer I, belongs to a novel family of homodimeric and heterodimeric DNA-binding proteins. Mol. Cell Biol. *14*, 1230–1244.

Riddle, D.L., and Albert, P.S. (1997). Genetic and environmental regulation of dauer larva development. In *C. elegans* II, D.L. Riddle, T. Blumenthal, B.J. Meyer, and J.R. Priess, eds. (Cold Spring Harbor, NY: Cold Spring Harbor Laboratory Press), pp. 739–768.

Roayaie, K., Crump, J.G., Sagasti, A., and Bargmann, C.I. (1998). The G alpha protein ODR-3 mediates olfactory and nociceptive function and controls cilium morphogenesis in *C. elegans* olfactory neurons. Neuron *20*, 55–67.

Rosenbaum, J.L., Cole, D.G., and Diener, D.R. (1999). Intraflagellar transport: the eyes have it. J. Cell Biol. *144*, 385–388.

Ruvkun, G. (1997). Patterning the nervous system. In *C. elegans* II, D.L. Riddle, T. Blumenthal, B.J. Meyer, and J.R. Priess, eds. (Cold Spring Harbor, NY: Cold Spring Harbor Laboratory Press), pp. 543–581.

Sambrook, J., Fritsch, E.F., and Maniatis, T. (1989). Molecular cloning: a laboratory manual, 2nd Edition (Cold Spring Harbor, NY: Cold Spring Harbor Laboratory Press).

Scalettar, B.A., Swedlow, J.R., Sedat, J.W., and Agard, D.A. (1996). Dispersion, aberration and deconvolution in multi-wavelength fluorescence images. J. Microsc. *182*, 50–60.

Sengupta, P., Chou, J.H., and Bargmann, C.I. (1996). *odr-10* encodes a seven transmembrane domain olfactory receptor required for responses to the odorant diacetyl. Cell *84*, 899–909.

Signor, D., Wedaman, K.P., Orozco, J.T., Dwyer, N.D., Bargmann, C.I., Rose, L.S., and Scholey, J.M. (1999a). Role of a class DHC1b dynein in retrograde transport of IFT motors and IFT raft particles along cilia, but not dendrites, in chemosensory neurons of living *Caenorhabditis elegans*. J. Cell Biol. *147*, 519–530.

Signor, D., Wedaman, K.P., Rose, L.S., and Scholey, J.M. (1999b). Two heteromeric kinesin complexes in chemosensory neurons and sensory cilia of *Caenorhabditis elegans*. Mol. Biol. Cell *10*, 345–360.

Starich, T.A., Herman, R.K., Kari, C.K., Yeh, W.H., Schackwitz, W.S., Schuyler, M.W., Collet, J., Thomas, J.H., and Riddle, D.L. (1995). Mutations affecting the chemosensory neurons of *Caenorhabditis elegans*. Genetics *139*, 171–188.

Stephens, R.E. (1995). Ciliogenesis in sea urchin embryos—a subroutine in the program of development. Bioessays *17*, 331–340.

Sulston, J.E., and Horvitz, H.R. (1977). Post-embryonic cell lineages of the nematode, *Caenorhabditis elegans*. Dev. Biol. *56*, 110–156.

Sulston, J.E., Schierenberg, E., White, J.G., and Thomson, J.N. (1983). The embryonic cell lineage of the nematode *Caenorhabditis elegans*. Dev. Biol. *100*, 64–119.

Tabish, M., Siddiqui, Z.K., Nishikawa, K., and Siddiqui, S.S. (1995). Exclusive expression of *C. elegans osm-3* kinesin gene in chemosensory neurons open to the external environment. J. Mol. Biol. *247*, 377–389.

Thompson, J.D., Higgins, D.G., and Gibson, T.J. (1994). CLUSTAL W: improving the sensitivity of progressive multiple sequence alignment through sequence weighting, position-specific gap penalties and weight matrix choice. Nucleic Acids Res. *22*, 4673–4680.

Troemel, E.R., Chou, J.H., Dwyer, N.D., Colbert, H.A., and Bargmann, C.I. (1995). Divergent seven transmembrane receptors are candidate chemosensory receptors in *C. elegans*. Cell *83*, 207–218.

Ward, S., Thomson, N., White, J.G., and Brenner, S. (1975). Electron microscopical reconstruction of the anterior sensory anatomy of the nematode *Caenorhabditis elegans*. J. Comp. Neurol. *160*, 313–337.

Ware, R.W., Clark, D., Crossland, K., and Russell, R.L. (1975). The nerve ring of the nematode *Caenorhabditis elegans*: sensory input and motor output. J. Comp. Neurol. *162*, 71–110.

White, J.G., Southgate, E., Thomson, J.N., and Brenner, S. (1986). The structure of the nervous system of the nematode *Caenorhabditis elegans*. Philos. Trans. R. Soc. Lond. B. Biol. Sci. *314*, 1–340.

Wicks S.R., de Vries C.J., van Luenen, H.G.A.M., and Plasterk, R.H.A.P. (2000). CHE-3, a cytosolic dynein heavy chain, is required for sensory cilia structure and function in C. elegans. Dev. Biol., *in press.*

Wu, S.Y., and McLeod, M. (1995). The sak1+ gene of *Schizosaccharomyces pombe* encodes an RFX family DNA-binding protein that positively regulates cyclic AMP-dependent protein kinase-mediated exit from the mitotic cell cycle. Mol. Cell Biol. *15*, 1479–1488.

Yu, S., Avery, L., Baude, E., and Garbers, D.L. (1997). Guanylyl cyclase expression in specific sensory neurons: a new family of chemosensory receptors. Proc. Natl. Acad. Sci. USA *94*, 3384–3387.

Zipursky, S.L., and Rubin, G.M. (1994). Determination of neuronal cell fate: lessons from the R7 neuron of *Drosophila*. Annu. Rev. Neurosci. *17*, 373–397.

GenBank Accession Numbers

The alternatively spliced *daf-19* sequences reported in this paper have the GenBank accession numbers AF226156 and AF233652.

Note Added in Proof

Recently, a *Drosophila* RFX homolog (dRFX) that is expressed in the peripheral nervous system and in the brain has been reported: Durand, B., Vandaele, C., Spencer, D., Pantalacci, S., and Couble, P. (2000). Cloning and characterization of dRFX, the *Drosophila* member of the RFX family of transcription factors. Gene, in press.